J. Eukaryot. Microbiol., 53(6), 2006 pp. 407–419

DOI: 10.1111/j.1550-7408.2006.00124.x

Two New Species of Symbiotic Ciliates from the Respiratory Tract of Cetaceans with Establishment of the New Genus *Planilamina* n. gen. (Dysteriida, Kyaroikeidae)

HONGWEI MA,[a] ROBIN M. OVERSTREET,[a] JAMES H. SNIEZEK,[b] MOBASHIR SOLANGI[c] and D. WAYNE COATS[d]

[a]*Department of Coastal Sciences, The University of Southern Mississippi, 703 East Beach Drive, Ocean Springs, Mississippi 39564, and*
[b]*Department of Biology, Montgomery College, 51 Mannakee Street, Rockville, Maryland 20850, and*
[c]*Institute for Marine Mammal Studies, PO Box 207, Gulfport, Mississippi 39502, and*
[d]*Smithsonian Environmental Research Center, PO Box 28, Edgewater, Maryland 21037, USA*

ABSTRACT. Examination of mucus discharged from the blowhole of Atlantic bottlenose dolphin (*Tursiops truncatus*) at Marine Life Oceanarium, Gulfport, Mississippi, and false killer whale (*Pseudorca crassidens*) and Atlantic bottlenose dolphin at SeaWorld Orlando, Orlando, Florida, using live observations and protargol impregnation revealed mixed infections of *Kyaroikeus cetarius* and two new species. *Planilamina* n. gen. is characterized by a C-shaped argentophilic band located along the laterally flattened margin of cell and extending from the cell apex to subposterior cone-shaped podite; a deep oral cavity containing one short preoral kinety, two circumoral kineties, seven to 13 infundibular kineties, and a cytostome; a broadly funnel-shaped cytopharynx reinforced by argentophilic fibers but without nematodesmata; closely packed postoral kinetofragments set in a pocket located anterior left of the podite; and somatic kineties as a right field closely situated at the right surface and a left field bordering the anterior left margin of the oral cavity. The type species for the genus, *Planilamina ovata* n. sp., is distinguished from its sister species *Planilamina magna* n. sp. by the following characteristics: body size (28–65 × 20–43 μm vs. 57–90 × 40–63 μm), number of right field kineties (38–55 vs. 79–99), and position of the anterior end of the leftmost kinety in the right somatic field (anterior one-third vs. mid-body). The morphogenesis of *Planilamina ovata* is similar to that of *K. cetarius*. The diagnosis of Kyaroikeidae is emended to accommodate the new genus.

Key Words. Ciliophora, dolphin, morphogenesis, morphology, *Planilamina magna* n. sp., *Planilamina ovata* n. gen., n. sp., *Pseudorca crassidens*, *Tursiops truncatus*, whale.

RESEARCH on protozoa from cetaceans is sparse primarily because of the challenges of sample collection. Difficulties involve the relative inaccessibility of wild hosts and complicated protocols for collection (Dailey 1985; Poynton, Whitaker, and Heinrich 2001). Protozoa, namely apicomplexans, flagellates, and ciliates, have been reported from marine mammals. Among the Apicomplexa, *Sarcocystis* infections have been discovered in the Pacific harbor seal (*Phoca vitulina richardsi*) (Lapointe et al. 1998), beluga whale (*Delphinapterus leucas*) (DeGuise et al. 1993), Atlantic white-sided dolphin (*Lagenorhynchus acutus*) (DeGuise et al. 1993; Ewing et al. 2002), and striped dolphin (*Stenella coeruleoalba*) (Resendes et al. 2002b). By contrast, *Toxoplasma* infections have been reported from the estuarine dolphin *Sotalia guianensis* (Bandoli and Oliverira 1977), spinner dolphin (*Stenella longirostris*) (Migaki, Sawa, and Dubey 1990), Atlantic bottlenose dolphin (*Tursiops truncatus*) (Cruickshank et al. 1990), striped dolphin (Domingo et al. 1992), beluga whale (Mikaelian et al. 2000), Indo-Pacific bottlenose dolphin (*Tursiops aduncus*) (Jardine and Dubey 2002), Risso's dolphin (*Grampus griseus*) (Resendes et al. 2002a), Indo-Pacific humpbacked dolphin (*Sousa chinensis*) (Bowater et al. 2003), as well as harp seal (*Phoca groenlandica*), ringed seal (*Phoca hispida*), hooded seal (*Cystophora cristata*), and minke whale (*Balaenoptera acutorostrata*) (Oksanen et al. 1998). Dubey et al. (2003), who treated *Neospora caninum* in marine mammals, also provided additional references for marine mammal infections with species of *Sarcocystis* and *Toxoplasma*. Only one flagellate species, the bodonid *Jarrellia atramenti* from the respiratory tract of the pygmy sperm whale, has been well described (Poynton et al. 2001).

Reported ciliates include the following: the prostomatean ciliate *Haematophagus megrapterae* from baleen plates of humpback whale (*Megaptera novaeangliae*), fin whale (*Balaenoptera physalus*), and blue whale (*Balaenoptera musculus*) (Evans, Small, and Snyder 1986; Woodcock and Lodge 1921); the dysteriid *Kyaroikeus cetarius* from the blowhole, alveolar spaces, and sub-bronchial mucosa of the killer whale (*Orcinus orca*), false killer whale (*Pseudorca crassidens*), pygmy killer whale (*Feresa attenuata*), Atlantic spotted dolphin (*Stenella frontalis*), bottlenose dolphin (*T. truncatus*), Fraser's dolphin (*Lagenodelphis hosei*), short-beaked common dolphin (*Delphinus delphis*), and beluga whales (Poynton et al. 2001; Schulman and Lipscomb 1997, 1999; Sniezek and Coats 1996; Sniezek, Coats, and Small 1995; Sweeney and Reddy 2001; Woodard et al. 1969); and unidentified ciliates from the blowhole, skin lesions, lymph nodes, and bronchioli (Dailey 1985; Howard, Britt, and Matsumoto 1983; Poynton et al. 2001; Schulman and Lipscomb 1997, 1999). The unidentified ciliate, found in the blowhole of Atlantic bottlenose dolphin from Hawaii and California described as a broad-bodied ciliate tentatively identified as a phyllopharyngid (chilodonellid) ciliate (Dailey 1985; Poynton et al. 2001), differs from that which we describe here (Poynton, pers. commun.).

Of the ciliates associated with the respiratory tract of Atlantic bottlenose dolphin, we have seen *K. cetarius*, the only described species of the genus. We have also seen four previously undescribed ciliates, one belonging to *Kyaroikeus*, a chilodonellid to be described by Poynton and colleagues (Poynton, pers. commun.) and two not assignable to a known genus. In this paper, we describe a new genus related to *Kyaroikeus* to accommodate the latter two new species.

MATERIALS AND METHODS

Samples were collected from trained Atlantic bottlenose dolphins at Marine Life Oceanarium, Gulfport, MS, during 2002–2003, from the Atlantic bottlenose dolphins and false killer whale at SeaWorld, FL, USA in 1994 and 1997, and from necrotic Atlantic bottlenose dolphins washed ashore at Virginia Beach, VA during June 1987. Nasal mucus obtained from living hosts by force exhalation was collected on either an apparatus holding six slides together or a Petri dish approximately 10–15 cm above the blowhole of the animal. A total of three to four force exhalations were accomplished from each dolphin by gently tapping it 2–3 cm anterior to the blowhole after the dolphin had been encouraged to

Corresponding Author: R. Overstreet, Gulf Coast Research Laboratory, 703 East Beach Drive, Ocean Springs, MS 39564—Telephone number: +1 228 872 4243; FAX number: +1 228 872 4204; e-mail: robin.overstreet@usm.edu

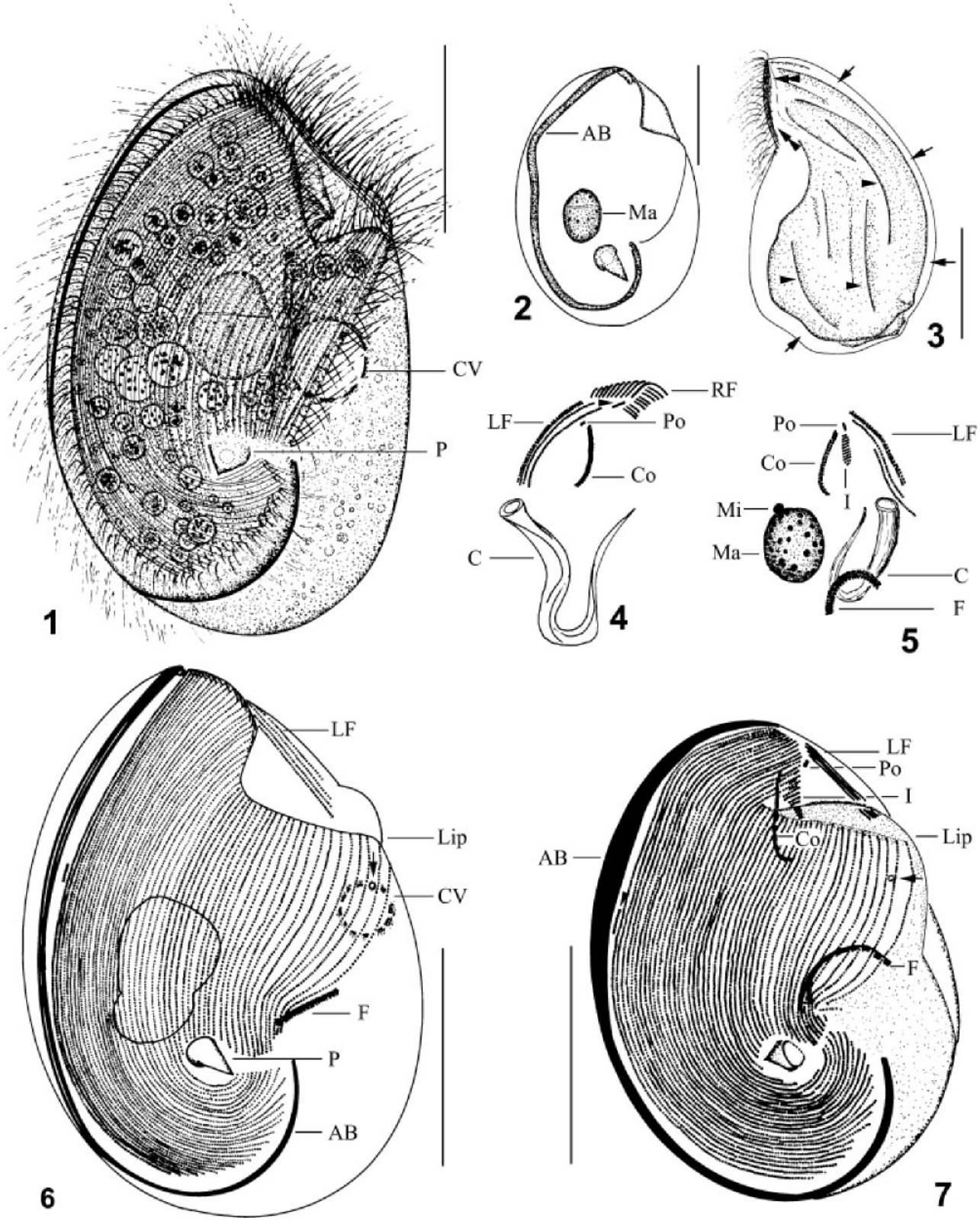

Fig. **1–7.** *Planilamina ovata* n. gen., n. sp., from life (1, 3) and after protargol impregnation (2, 4–7). **1.** Right view of typical individual. **2.** Right view, showing the argentophilic band and podite. **3.** Left view, arrows indicate the C-shaped bright groove, arrowheads show the short grooves on surface, and double arrowheads point to the anterior kineties of right field turning over to dorsal side. **4.** Left view of oral region, arrowhead indicates CDE (cinétie droite externe) anterior. **5.** Right view of oral region. **6–7.** Right views of infraciliature, arrowhead indicates the CDE, and arrow points to the contractile vacuole pore. AB, argentophilic band; C, cytopharynx; Co, circumoral kineties; CV, contractile vacuole; F, postoral kinetofragments; I, infundibular kineties; LF, left field; Ma, macronucleus; Mi, micronucleus; P, podite; Po, preoral kineties; RF, right field. Scale bars = 20 μm.

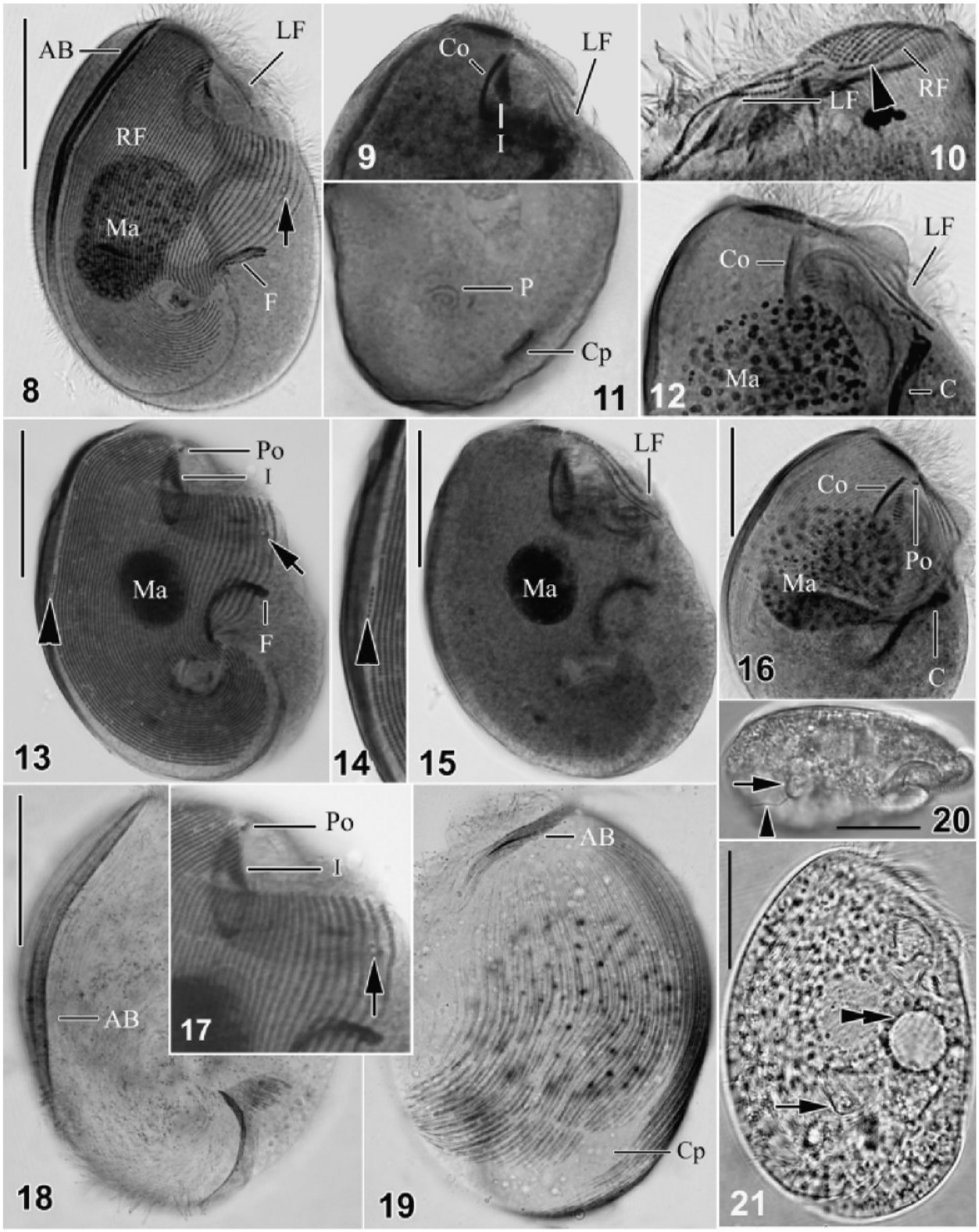

Fig. **8–21.** Photomicrographs of *Planilamina ovata* after protargol impregnation (8–19) and from life (20–21). **8.** Right view, with arrow indicating the contractile vacuole pore. **9, 12.** Oral region. **10.** Left view, showing the anterior ends of rightmost 8–11 kineties in right field, left field kineties and CDE anterior (arrowhead). **11.** Left view of the posterior end, showing the slit-like cytoproct and base of podite. **13–15, 17.** Same individual, showing the left and right field kineties, preoral kinety, CDE (arrowhead), contractile vacuole pore (arrow), and postoral kinetofragments. **16.** Preoral kinety, circumoral kineties, left field kineties, and cytopharynx. **18, 19.** Right and left view of the same individual, showing the C-shaped argentophilic band, very fine non-ciliated tracts, and cytoproct. **20.** Lateral view, arrowhead indicates attachment thread emanating from tip of podite, arrow shows podite. **21.** Typical individual showing podite (arrow) and contractile vacuole (double arrows). AB, argentophilic band; C, cytopharynx; Co, circumoral kineties; CV, contractile vacuole; Cp, cytoproct; F, kinetofragments; I, infundibular kineties; LF, left field; Lip, Ma, macronucleus; Mi, micronucleus; P, podite; Po, preoral kineties; RF, right field. Scale bars = 20 μm.

rest with its head or body out of the water along the side of a pool. The Petri dishes were immediately covered and taken to the laboratory for observations of live organisms. Stained preparations were made using protargol impregnation according to the method of Wilbert (1975) and the quantitative protargol stain (QPS) method following Montagnes and Lynn (1993). Nasal swabs of necrotic hosts were preserved on site and taken to the laboratory for QPS. The specimens were photographed and measured using Zeiss or Olympus optics and an Evolution MP 5.0 RTV digital camera system.

RESULTS

Planilamina ovata n. sp. (Fig. 1–21, Table 1)

Description. Individuals of *Planilamina ovata* were usually detected in mucus samples along with host epithelia. The ciliates died within 1–2 h after leaving a host when maintained at room temperature in mucus samples or diluted in seawater. Locomotion occurred slowly in host mucus, with individuals often attaching to the substratum by their podite and rotating through the viscous medium while the cilia beat in a regular pattern. Cells swam more

Table 1. Morphometric data for two species of *Planilamina* n. gen. from cetacean hosts.

Character	Min	Max	Mean	Median	SD	SE	CV	n
Body length (μm)	57.0	90.0	72.3	72.2	9.20	1.78	12.8	27
	35.0	65.0	49.5	48.6	7.30	1.03	14.7	50
	27.7	59.8	46.9	47.6	7.58	1.16	16.2	43
Body width (μm)	40.0	63.0	52.6	54.2	6.00	1.15	11.4	27
	25.0	42.0	33.4	33.3	4.45	0.63	13.3	50
	19.9	42.7	33.0	33.2	5.21	0.80	15.8	43
Distance from cell apex to preoral kinety (μm)	10.0	20.0	13.9	13.9	2.72	0.52	19.6	27
	6.0	13.0	8.7	8.3	1.88	0.27	21.7	50
	—	—	—	—	—	—	—	—
Distance from cell apex to anterior end of circumoral kineties (μm)	10.0	19.0	13.4	13.2	2.49	0.48	18.5	27
	6.0	13.0	8.4	8.3	1.61	0.23	19.0	50
	—	—	—	—	—	—	—	—
Length of circumoral arch (μm)	4.0	9.0	6.9	6.9	1.24	0.24	18.0	27
	4.0	9.0	7.3	7.3	1.07	0.15	14.7	50
	5.5	8.9	7.2	7.7	0.90	0.22	12.5	17
Width of circumoral arch (μm)	3.0	10.0	5.8	5.6	1.44	0.28	25.0	27
	3.0	10.0	4.6	4.2	1.48	0.21	32.2	50
	—	—	—	—	—	—	—	—
Distance from cell apex to anterior end of left field (μm)	6.0	15.0	10.1	10.1	2.89	0.57	28.7	26
	3.0	11.0	6.7	6.9	2.00	0.29	29.8	49
	—	—	—	—	—	—	—	—
Length of left field (μm)	14.0	22.0	16.4	15.3	2.23	0.44	13.6	26
	10.0	20.0	15.8	16.0	2.31	0.33	14.7	49
	7.4	15.5	11.3	11.1	3.31	1.66	29.3	4
Distance from cell apex to anterior end of postoral kinetofragments (μm)	31.0	49.0	40.0	40.3	5.59	1.11	14.0	25
	22.0	44.0	29.1	28.5	5.03	0.74	17.2	46
	—	—	—	—	—	—	—	—
Length of postoral kinetofragments (μm)	3.0	18.0	11.1	11.8	3.85	0.77	34.5	25
	1.0	14.0	6.8	6.9	3.00	0.45	44.1	44
	4.4	10.0	6.6	6.6	1.50	0.29	22.7	26
Distance from cell apex to tip of podite (μm)	35.0	60.0	48.1	48.6	7.16	1.38	14.9	27
	24.0	49.0	36.0	35.4	6.54	0.92	18.2	50
	22.2	42.1	33.4	33.3	4.96	0.88	14.9	32
Width of podite (μm)	4.0	7.0	5.3	5.6	0.66	0.13	12.5	26
	4.0	6.0	4.3	4.2	0.72	0.11	16.9	45
	—	—	—	—	—	—	—	—
Length of macronucleus (μm)	8.0	23.0	16.3	16.7	3.38	0.74	20.8	21
	6.0	22.0	11.2	11.1	3.17	0.51	28.2	39
	6.6	18.8	12.6	12.2	2.73	0.43	21.7	40
Width of macronucleus (μm)	9.0	17.0	12.4	12.5	1.87	0.41	15.1	21
	5.0	14.0	8.0	8.3	1.85	0.30	23.2	39
	5.5	14.4	9.1	8.3	2.45	0.39	26.9	40
Distance from cell apex to posterior curvature of cytopharynx (μm)	30.0	51.0	42.4	43.7	6.01	1.20	14.2	25
	26.0	44.0	34.3	34.7	4.37	0.62	12.7	49
	—	—	—	—	—	—	—	—
Distance from cell apex to anterior margin of cytoproct (μm)	44.0	69.0	59.3	62.8	9.06	2.86	15.3	10
	26.0	47.0	36.9	34.7	8.71	3.89	23.6	5
	—	—	—	—	—	—	—	—
Cytoproct length (μm)	4.0	8.0	5.1	4.9	1.14	0.36	22.4	10
	3.0	6.0	4.7	5.6	1.24	0.56	26.3	5
	5.0	7.0	6.0	5.5	0.57	0.16	9.5	12

Table 1. (Continued).

Character	Min	Max	Mean	Median	SD	SE	CV	n
Number preoral kineties	1	1	1.0	1.0	0.00	0.00	0.0	27
	1	2	1.0	1.0	0.14	0.02	13.9	50
	1	1	1.0	1.0	0.00	0.00	0.0	10
Number circumoral kineties	2	2	2.0	2.0	0.00	0.00	0.0	27
	2	2	2.0	2.0	0.00	0.00	0.0	50
	2	2	2.0	2.0	0.00	0.00	0.0	50
Number infundibular kineties	3	13	10.0	10.0	2.21	0.48	22.1	21
	7	13	9.9	10.0	1.30	0.20	13.1	44
	7	13	10.2	10.0	1.81	0.57	17.7	10
Number right field kineties[a]	79	99	88.1	88.0	4.64	0.89	5.3	27
	38	55	45.4	46.0	4.35	0.61	9.4	50
	41	51	45.7	45.0	3.02	0.78	6.6	15
Number left field kineties	3	4	3.1	3.0	0.32	0.06	10.3	27
	3	4	3.1	3.0	0.30	0.04	9.8	50
	3	4	3.8	4.0	0.44	0.12	11.6	13
Number postoral kinetofragments	2	8	3.7	3.0	1.39	0.30	37.9	21
	2	6	3.7	3.0	1.24	0.20	33.9	39
	3	4	3.3	3.0	0.45	0.11	13.6	16
CDE posterior: number kinetosomes	3	9	5.6	6.0	2.15	0.81	37.9	7
	2	15	6.1	5.5	3.63	0.97	59.7	14
	4	10	6.1	6.0	0.71	0.18	11.6	16
Number chambers in secretory organelle complex	8	14	11.9	12.0	1.32	0.31	11.1	18
	7	14	10.0	9.5	3.16	1.58	31.6	4
	—	—	—	—	—	—	—	—

[a]Excluding CDE.

First line, *Planilamina magna* after QPS; second line, *Planilamina ovata* after quantitative protargol stain (QPS); third line, *Planilamina ovata* after Wilbert's protargol impregnation. CV, coefficient of variation; Max, maximum; Mean, arithmetic mean; Min, minimum; SD, standard deviation; SE, standard error; CDE, cinétie droite externe.

freely after being transferred to mucus diluted with seawater. *Planilamina ovata* generally maintained a discoid or ovate profile in life, with an obvious laterally flattened body shape. The cytoplasm was transparent and granular in appearance, often containing numerous well-defined food vacuoles. Food vacuoles usually contained unidentified amorphous material, but some included probable host epithelia.

The body was 28–65 × 20–43 μm in fixed specimens and 35–70 × 30–49 μm in vivo, with ratio of length to width about 3:2. The right side of the cell was flat and the left side slightly convex, with the anterior end slightly pointed and the posterior margin bluntly rounded (Fig. 1, 3, 20, 21). A C-shaped band (or groove) delineating the non-ciliated left side from the ciliated right side ran anterior to posterior along the narrow dorsal margin, curved around the posterior end, and extended anteriorly onto the left side of the cell. This structure was clearly visible in vivo as a deep bright groove and in protargol-impregnated specimens as an argentophilic band (AB) (Fig. 1–3, 6–8, 13, 18). Several shallow furrows were also found in the middle of the left surface (Fig. 3, arrowheads) and appeared in vivo as irregular furrows and ridges. In protargol-impregnated specimens, the non-ciliated left surface had 35–45 very fine tracks aligned anterior to posterior (Fig. 19).

Body ciliature was primarily restricted to the right surface, with cilia about 8 μm long and densely spaced monokinetids within kineties. Somatic kineties of the right field numbered 38–55, the leftmost 15–23 being short and running anteriorly to the oral region. The leftmost kinety of the right field originated at the anterior one-third of the cell and terminated at the anterior margin of the podite. The remaining right field kineties originated anteriorly from the oral area and extended to the level of the podite before curving sinistrally. The anterior end of the rightmost 8–11 kineties of the right field turned over to the dorsal surface (Fig. 3, double arrowheads, 4, 10). Non-ciliated kinetosomes ranging in number from 2 to 15 (usually six) were located equatorially as a short row (cinétie droite externe, CDE in Deroux and Dragesco 1968) between the C-shaped argentophilic band and the rightmost kinety in the right field (Fig. 6, 7, 13, 14, arrowhead). Another short kinetofragment was located adjacent to the argentophilic band at the anterior ends of rightmost five kineties in the right field (considered CDE anterior in Fig. 4; 10, arrowhead). Left field kineties numbered 3–4, originated near the anterior end of the argentophilic band, and terminated posteriorly at the level of the cytostome (Fig. 4–10, 15, 16). Two to six (usually four) postoral kinetofragments consisting of short rows of densely packed kinetosomes were situated in a ventral pocket located anterior to the podite and often curved to the right (Fig. 5–8, 13).

Somatic cilia located around the oral region beat anteriorly in vivo (Fig. 1, 8). The oral apparatus (details apparent in well-impregnated specimens only because structures were deeply situated in an oral depression) typically consisted of a preoral kinety, two circumoral kineties, seven to 13 infundibular kineties, and the cytostome. The preoral kinety (very rarely two were present) was composed of one or two closely set kinetosomes (Fig. 4, 5, 7, 13, 16, 17). The circumoral kineties ran parallel to each other, originated posterior and to the right of the preoral kinety, and coursed posteriad as a tight arc, with the posterior end forming a hook (Fig. 4, 5, 7, 9, 12). The infundibular kineties derived from the anterior ends of right field kineties and curved into the oral depression anterior of the cytostome (Fig. 7, 9, 17).

The subterminal podite was broadly cone-shaped, measuring 5–6 μm long, with the base being about 4–6 μm wide (Fig. 1, 2, 6, 7, 20, 21). A secretory organelle complex (SOC) was positioned beneath the podite and composed of seven to 14 chambers forming a conical spiral that rotated sinistrally about two and one-half circles to the podite. An attachment thread (Fig. 20, arrowhead) extended from the tip of the podite when seen in vivo and usually

connected with a host cell. The cytoproct occurred as a slit or wide depression opening as a groove on the posterior left surface (Fig. 11, 19). The broad oral region was located anteriorly and had two distinct lips protruding externally (Fig. 6, 7, 12, 16). The cytostome was located posteriad in the oral region, leading to a cytopharynx (Fig. 4, 5) lacking nematodesmata, but strongly reinforced by argentophilic ribbons that extended beyond the cell equator before turning sharply anteriad. A single contractile vacuole measuring 3–6 μm in diam. was positioned adjacent to the cytostome, with the contractile vacuole pore (CVP) located anteriorly between the second and third kinety of the right field (Fig. 6, 8, 13, arrow).

The heteromeric macronucleus was ovoid, centrally situated in the body, and associated with an adjacent ellipsoid micronucleus (Fig. 1, 5, 6, 8, 13, 16).

Morphogenesis (Fig. 22–27). Specimens in morphogenetic stages were rare in host nasal mucus relative to those of *K. cetarius*. The parental cytopharynx during cell division was partially to completely replaced, accompanied by elaboration of a new cytopharynx beneath the parental circumoral kineties. The overall morphogenetic process was similar to that of *K. cetarius* and is presented below as five stages.

Stage 1 (Fig. 22A, 23): Replication of kinetosomes within postoral kinetofragments, development of three to four new kinetal fragments. Morphogenesis commenced with the proliferation of postoral kinetofragments within the ventral pocket and immediately to left of the more dorsally positioned parental fragments. A total of seven to eight kinetofragments thus lined the dorsal and left wall of the ventral pocket. For clarity, the kinetofragments are numbered sequentially from right to left, with the three (sometimes four) new rows (kf5–kf7) slightly separated from and shorter than the original fragments (kf1–kf4). All seven kinetofragments increased in length by replication of kinetosomes within each row.

Stage 2 (Fig. 22B): Dorsal recession of kinetofragments with allometric growth of ventral depression. As the seven kinetofragments elongated, the ventral pocket expanded dorsally and increased in length to become a more furrow-shaped depression that deepened sharply along the anterior-dorsal wall causing the upper third of kf1–kf4 to curve dorsally. The second fragment (kf2) was most recessed and separated into a strongly curved anterior segment (kf2b) and a more linear posterior portion (kf2c). The newly formed kinetofragments (kf5–kf7) remained on the left wall of the furrow, with a gap between those fragments and kf1–kf4 widening anteriorly.

Stage 3 (Fig. 22C, 24, 25): Formation of anlagen for proter secretory organelle complex and somatic postoral fragments. The ventral furrow continued to invaginate, giving rise to the developing oral cavity of the opisthe. Anterior tips of kf1–kf4 broke

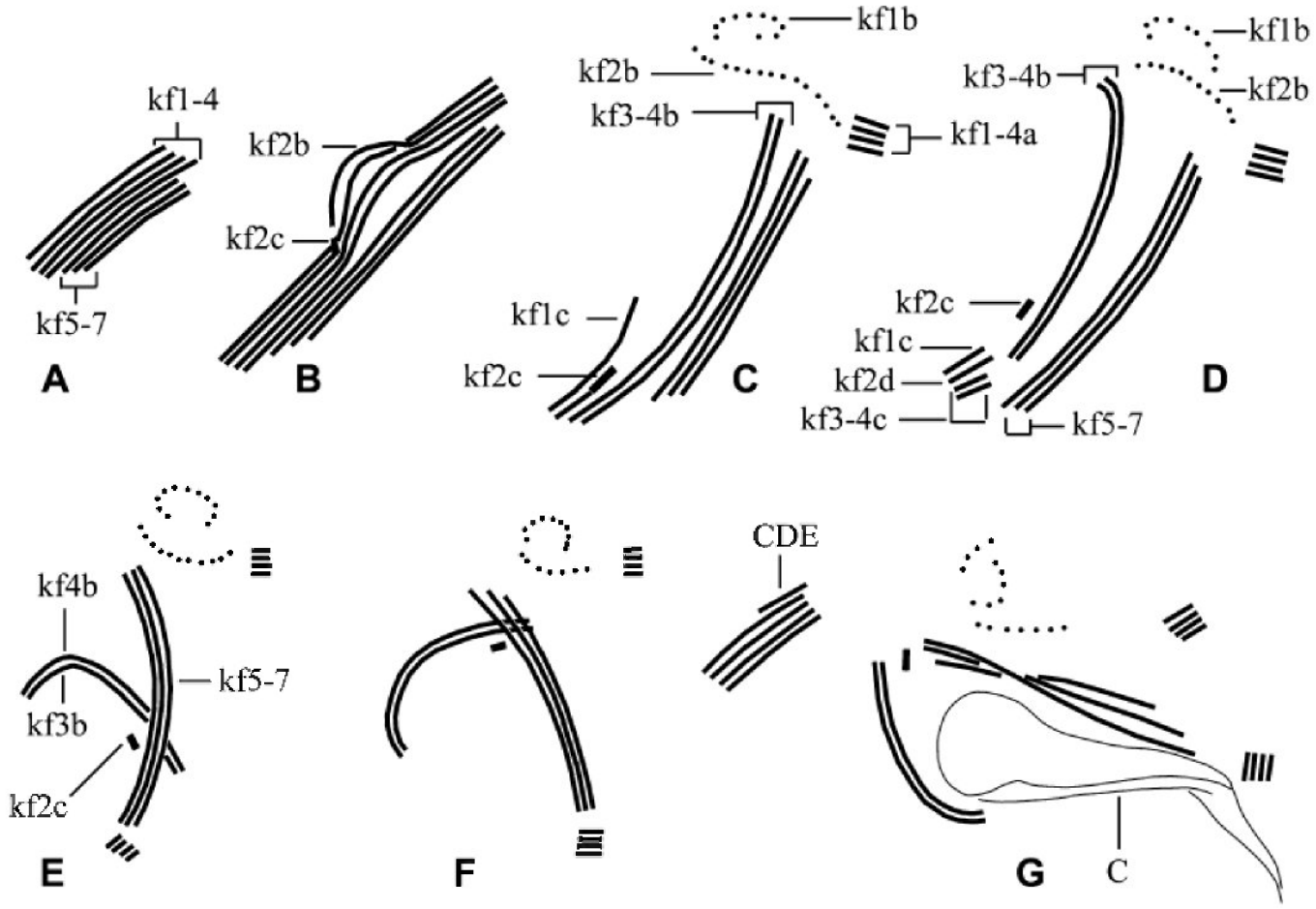

Fig. 22. Summary drawings of key morphogenetic stages in *Planilamina ovata* as revealed by protargol impregnation. (**A**) Stage 1, formation of three additional rows of kinetosomes (kf5–kf7) to the left of the parental kinetofragments (kf1–kf4). (**B**) Stage 2, dorsal recession of parental kinetofragments accompanied by fragmentation of kf2. (**C**) Stage 3, formation of anlage for the proter secretory organelle complex (kf1b, kf2b), separation of postoral kinetofragments (kf1–kf4a) for the proter, and counterclockwise migration of circumoral anlagen (kf3–kf4b). (**D**) Stage 4, formation of anlagen for opisthe preoral kinety (kf2c), circumoral kineties (kf3b, kf4b), and postoral kinetofragments (kf1c, kf2d, kf3–kf4c). (**E–G**) Stage 5, continued counterclockwise migration of opisthe preoral and circumoral kineties. C, cytopharynx; CDE, newly formed CDE (cinétie droite externe) anterior.

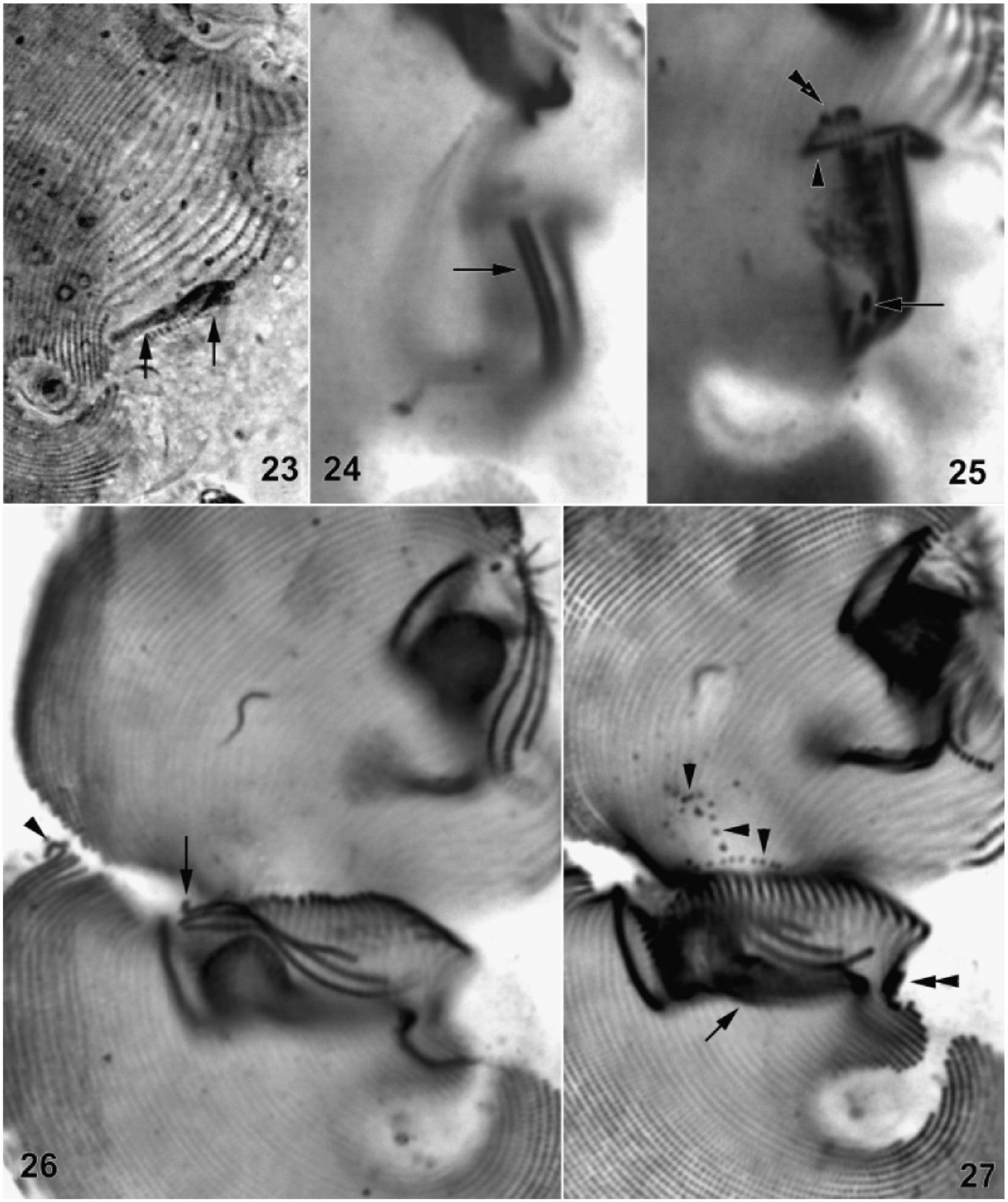

Fig. **23–27.** Morphogenesis in *Planilamina ovata* after protargol impregnation. **23.** Stage 1, arrows showing the newly formed kinetosomal rows. **24.** Stage 3, arrow illustrating the counterclockwise rotation of the circumoral kineties anlagen (kf3b, kf3b). **25.** Stage 3, arrowhead and double arrowheads indicating secretory organelle complex anlage kf1b and kf2b of proter, respectively, and arrow denoting preoral kinety anlage (kf3c) of opisthe. **26.** Stage 5, arrowhead indicating CDE anterior of opisthe, arrow showing preoral kinety. **27.** Stage 5, arrowheads illustrating the basal bodies of secretory organelle complex in proter, arrow showing cytopharynx, and double arrowheads pointing to postoral kinetofragments in opisthe.

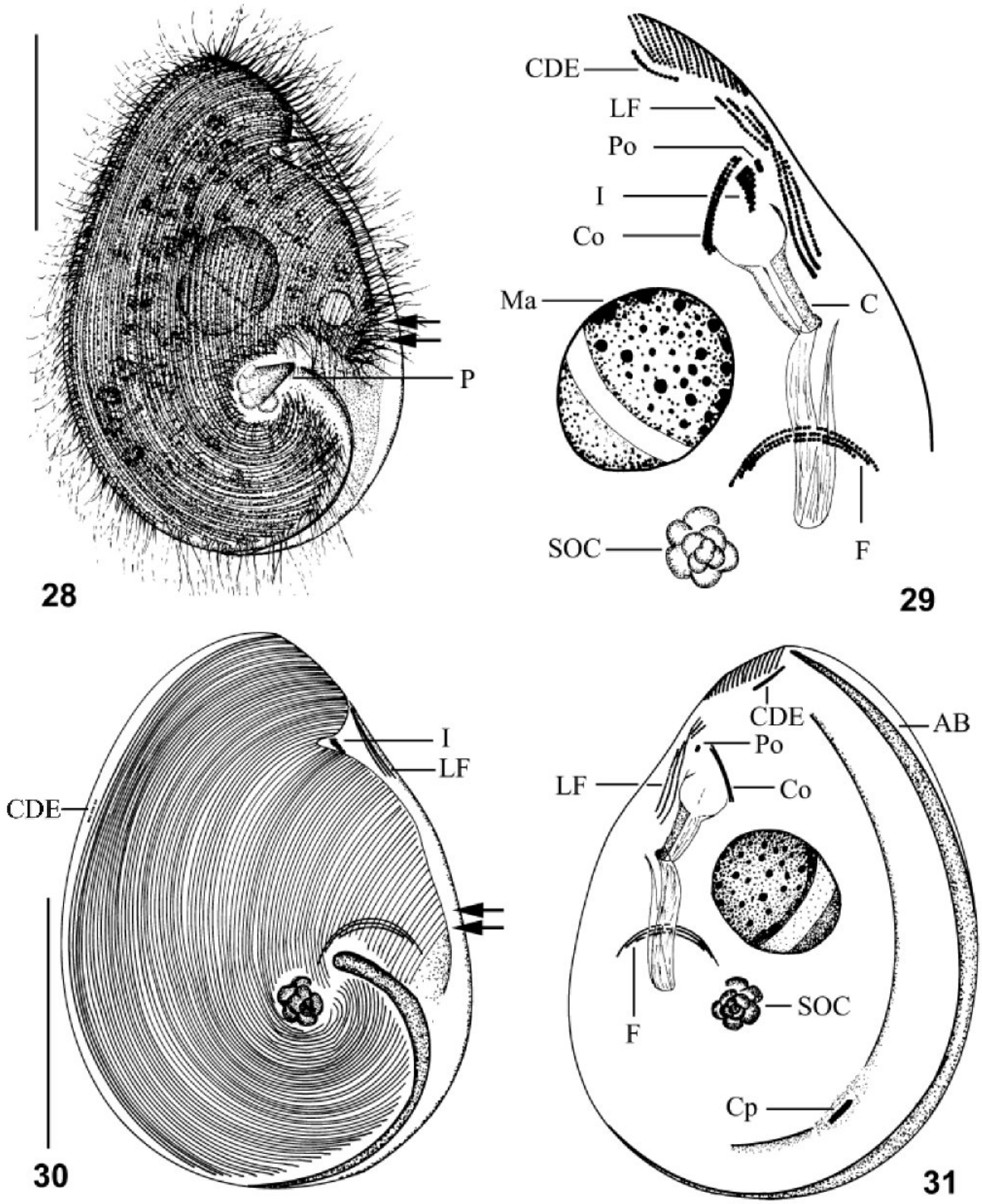

Fig. **28–31.** *Planilamina magna* n. sp., from life **(28)** and after protargol impregnation **(29–31). 28.** Right view of typical individual, arrows indicating the anterior of the leftmost kineties in right field. **29.** Right view of oral region. **30–31.** Right and left views of the same individual, arrows indicating the anterior of leftmost kineties in right field. AB, argentophilic band; C, cytopharynx; CDE, cinétie droite externe; Co, circumoral kineties; Cp, cytoproct; F, postoral kinetofragments; I, infundibular kineties; LF, left field; Ma, macronucleus; P, podite; Po, preoral kineties; SOC, secretory organelle complex. Scale bars = 30 μm.

free within the deepening of oral cavity, forming a group of four short kinetosomal rows (kf1a–kf4a), which slowly migrated anteriad to form the postoral kinetofragments for the proter. The posterior section of kf2b and a small portion of kf1 (kf1b) migrated anteriad and to the right, arranging sparsely and irregularly to form the anlage for the secretory organelle complex of the proter. Posterior segments of the parental kinetofragments (kf1c–kf2c and kf3b–kf4b) sank deeper into developing oral cavity, with two of these fragments (kf3b, kf4b) remaining closely associated, beginning to curve dorsally and to right as an anterior sinistral arc. Anterior ends of the leftmost kinetofragments (kf5–kf7) began to migrate to the right, accompanying development of opisthe oral cavity.

Stage 4 (Fig. 22D): Formation of anlagen for opisthe preoral kineties, circumoral kineties, and postoral kinetofragments. After starting their turn to the right, the third and fourth kinetofragments divided forming long anterior (kf3b and kf4b) and short posterior (kf3c and kf4c) segments. Kinetofragment kf2c also divided, producing a short anterior and a longer posterior (kf2d) segment. Simultaneously, kf1c reduced in length through resorption of anterior kinetosomes. The long parallel rows of kinetosomes from kf3b and kf4b and the small set of kinetosomes from kf2c generated the anlagen of the opisthe circumoral and preoral kineties, respectively. The four remnant fragments (kf1c, kf2d, kf3c and kf4c) formed the anlagen of the postoral kinetofragments. However, kinetofragments kf5–kf7 simultaneously generated the anlagen of the opisthe left field kineties.

Stage 5 (Fig. 22E–G, 26, 27): Counterclockwise migration of opisthe preoral and circumoral kineties. With continued enlargement of the oral cavity, its left wall invaginated beneath the developing left field kineties, gradually forcing those kineties toward the ventral surface. The anterior ends of the circumoral kineties formed a sinistral hook during this process, while the posterior tips simultaneously began to move anteriad in a counterclockwise rotation underneath the developing left field. The preoral kinety migrated along with the circumoral kineties so that by the end of Stage 5 (Fig. 22G, 26, 27) all three kineties had inverted. The cytopharynx also formed in this stage, with supporting microtubules contributed by the circumoral kineties.

During this morphogenetic process, the parental equatorial CDE proliferated to form three portions. The anterior and posterior sections developed into the equatorial CDEs of the proter and opisthe, respectively, while the middle section formed the anterior CDE of the opisthe (Fig. 22G, 26, arrowhead).

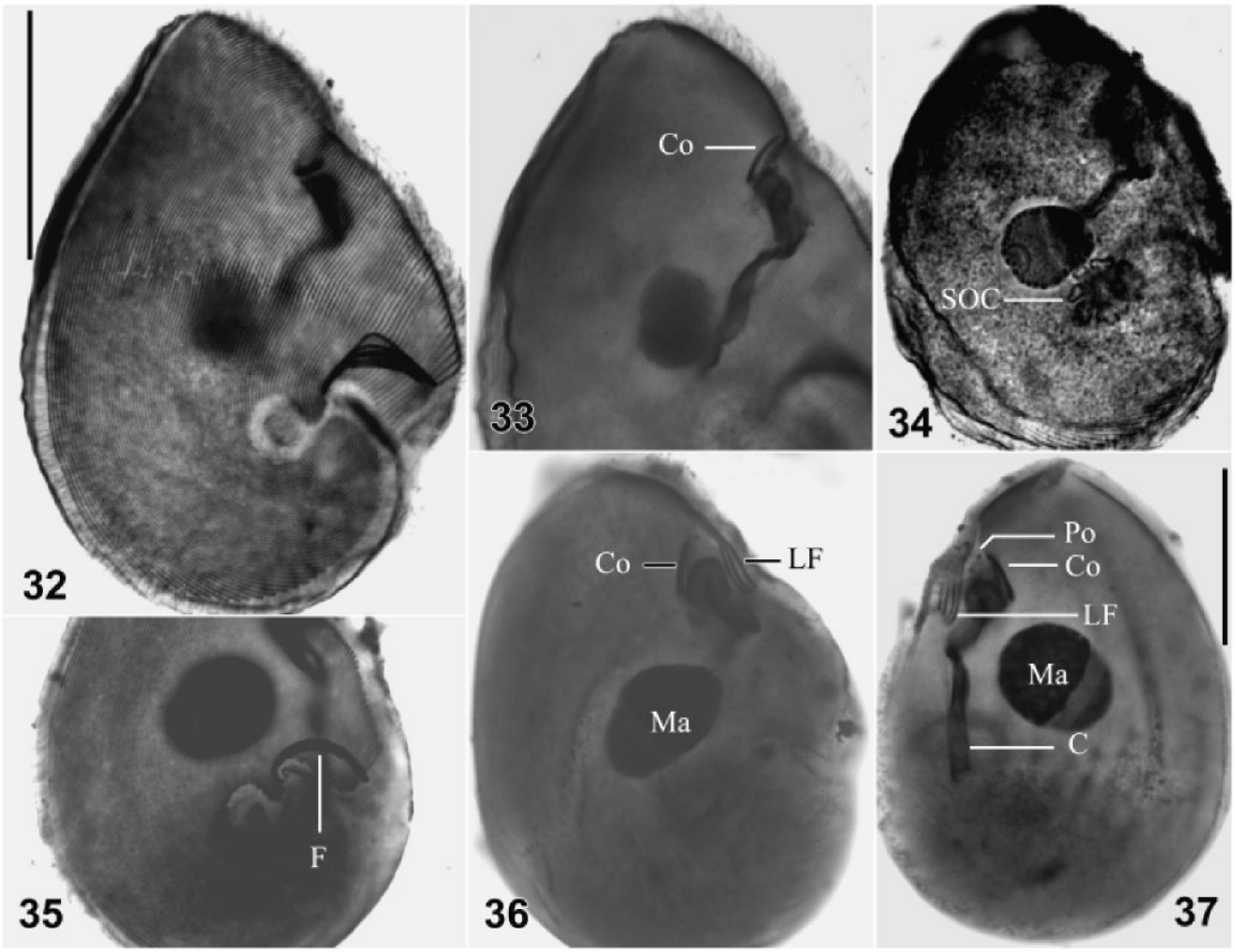

Fig. **32–37.** Photomicrographs of *Planilamina magna* after protargol impregnation. **32.** Right view, showing the arrangement of right field kineties. **33.** Oral region, illustrating circumoral kineties (Co). **34.** Showing the chambers in secretory organelle complex (SOC). **35.** Illustrating postoral kinetofragments (F). **36–37.** Right and left views of the same individual, showing circumoral kineties (Co), preoral kinety (Po), left field (LF), cytopharynx (C), and macronucleus (Ma). Scale bars = 30 μm.

Macronuclear replication bands occurred prior to the onset of morphogenesis and traversed the nucleus before the start of karyokinesis.

***Planilamina magna* n. sp. (Fig. 28–37, Table 1).**

Description. Habitat and behavior of *Planilamina magna* were similar to those of *Planilamina ovata*. The body was oval to slightly reniform, measuring 57–90 × 40–63 μm in stained specimens, with ratio of length to width about 3:2. Cells were laterally compressed forming left and right sides, with the anterior end slightly pointed and posterior end distinctly blunt. A C-shaped argentophilic band delineated the non-ciliated left side from ciliated right side and extended anteriorly onto the left side of the cell (Fig. 31, 32).

The right field was formed by 79–99 closely packed kineties, the left half being short with their anterior ends gradually shortening from the oral region to mid-body (Fig. 28, 30, arrows; 32) and their posterior ends terminating anterior and left of the podite. The remaining right field kineties originated anteriorly from the oral area and extended to the location of podite before curving sinistrally. The anterior ends of rightmost 13–20 kineties in the right field turned over to the left surface (Fig. 29).

The equatorial CDE consisted of three to nine (usually six) kinetosomes and the CDE anterior was located at the anterior ends of the rightmost kineties (Fig. 29). Left field kineties numbered three to four, originated near the anterior end of the argentophilic band, and terminated posteriad at the level of the cytostome (Fig. 29–31, 37).

The left side of the cell was non-ciliated, with a shallow groove paralleling the C-shaped argentophilic band, and a slit-like cytoproct located in the posterior one-third of the cell (Fig. 31, 37). The subterminal podite was broadly cone-shaped, with the base about 4–7 μm wide (Fig. 28). The SOC located beneath the podite was composed of eight to 14 chambers arranged as a conical sinistral spiral that rotated about $2\frac{1}{2}$ circles to the podite (Fig. 34).

The anteriorly located oral region was broad and contained a single preoral kinety, two circumoral kineties, three to 13 infundibular kineties, and the cytostome. The circumoral kineties were parallel, originated posterior and to the right of preoral kinety, and coursed posteriad as a tight arc (Fig. 29, 31, 33, 36). The infundibular kineties derived from the anterior ends of right field kineties and curving into the oral depression anterior of cytostome (Fig. 29). The postoral kinetofragments consisted of two to eight short rows of densely packed kinetosomes situated in the ventral pocket anterior to the podite and often curving to the right (Fig. 29–32, 35). The cytopharynx lacked nematodesmata and was strongly reinforced by argentophilic ribbons that extended beyond the cell equator before turning sharply anteriad.

The ovoid heteromeric macronucleus was situated centrally in the body (Fig. 28, 29, 31, 37).

DISCUSSION

Planilamina differs from *Kyaroikeus* by having members with a distinctively ovate shape, a C-shaped argentophilic band located along the laterally flattened margin of the cell, a curving right field distributed on the right side only, a subterminal podite, and a relatively wide non-ciliated left side (Table 2). *Planilamina* resembles *Kyaroikeus*, both in the Kyaroikeidae, by having members with a podite, a deep oral cavity, heteromeric macronucleus, two parallel circumoral kineties, and four closely packed postoral kinetofragments. Species in both genera infest the cetacean respiratory tract, and acquisition of ultrastructural and molecular data should more clearly define the relationship between the two genera. Thus, we establish a new genus and provide the following improved diagnosis for the Family Kyaroikeidae.

Order Dysteriida Deroux 1976

Family Kyaroikeidae Sniezek and Coats 1996

Emended diagnosis. Body circular in cross-section or laterally compressed; adhesive region (podite) at posterior tip or right posterior of cell; one preoral and two circumoral kineties in deep oral cavity; set of postoral kinetofragments located in a mid-ventral depression; opisthe oral and proter podital anlagen produced from parental kinetofragments during cell division but opisthe left field kineties arising from new kinetofragments proliferated to left of parental kinetofragments; symbionts of cetaceans; two genera recognized.

Table **2.** Comparison between *Planilamina* and *Kyaroikeus*.

Character	*Planilamina*	*Kyaroikeus*
Morphology		
Shape	Lateral compressed	Elongated
Right field kineties	C-shaped curving along right side	Bipolarly arranged
Left field kineties	Ciliated, relatively wide, along left of oral region	Ciliated, relatively narrow, along left of oral region
Preoral kinety	Very short	Very short
Circumoral kineties	Two curving kineties	Two curving kineties
Postoral kinetofragments	Equatorially located, 45°–90° angle to longitudinal axis	Equatorially located, parallel to longitudinal axis
Cytopharynx	Lacking nematodesmata, reinforced by argentophilic ribbons	Lacking nematodesmata, reinforced by argentophilic ribbons
Fibrous tracts	Widely distributed in left side	Narrowly distributed in ventral side
Macronucleus	Heteromeric, central situated	Heteromeric, central situated
Podite	Right side, subposterior end	Posterior end
Cytoproct	Dorsal or left side	Ventral side
Morphogenesis		
Opisthe preoral kinety	kf2	kf2
Opisthe circumoral kineties	kf3-kf4	kf3-kf4
Opisthe left field	kf5-kf7, rarely kf5-kf8	kf5-kf8
Opisthe cytopharynx	Circumoral anlagen	Circumoral anlagen
Proter secretory organelle complex	kf1-kf2	kf1-kf2
Proter and opisthe postoral kinetofragments	kf1-kf4	kf1-kf4
Proter oral apparatus	Unchanged	Unchanged
Proter cytopharynx	Partially to completely resorbed	Partially to completely resorbed

kfn, kinetofragments numbered sequentially from right to left.

Type genus. *Kyaroikeus* Sniezek, Coats, and Small, 1995

Planilamina n. gen.

Diagnosis. Argentophilic band C-shaped, located along laterally flattened margin of cell, extending from apex to subterminal cone-shaped podite; deep oral cavity containing one short preoral kinety, two circumoral kineties, several infundibular kineties, and cytostome; cytopharynx broadly funnel-shaped, reinforced by argentophilic fibers but without nematodesmata; postoral kinetofragments closely packed in ventral pocket anterior left of podite.

Type species. *Planilamina ovata* n. sp.

Etymology. The Latin "*Planilamina*," meaning flat (*plana*) and plate (*lamina*), is in feminine gender and refers to the flattened plate-like nature of members in the genus.

There are two species so far assigned to the new genus, the type species *Planilamina ovata* and its larger sister species, *Planilamina magna*. *Planilamina ovata* can be distinguished from *Planilamina magna* by the following characteristics: (1) body size (28–65 × 20–43 μm vs. 57–90 × 40–63 μm in protargol stained specimens); (2) number of right field kineties (38–55 vs. 79–99); and (3) position of the anterior end of the leftmost kinety in right field (anterior one third vs. mid-body).

From our observations, the species of *Planilamina* always accompanied the infestation of *K. cetarius* in the blowhole of cetaceans at Marine Life of Mississippi and Sea World of Florida. However, not only was the number of individuals of the species of *Planilamina* nearly one or two orders of magnitude fewer than that of *K. cetarius*, but the size of the cells was also smaller than that of *K. cetarius*. The smaller size and lower prevalence of *Planilamina* may be reasons these ciliates have not been previously reported. If co-occurrence of *Planilamina* and *Kyaroikeus* is common in cetaceans as our results suggest, then species of *Planilamina* may have a wide distribution among cetaceans in the Atlantic Ocean as well as in the Gulf of Mexico, particularly considering that *K. cetarius* has been found widely in dolphin and whale (Poynton et al. 2001; Schulman and Lipscomb 1997, 1999; Sniezek and Coats 1996; Sniezek et al. 1995; Sweeney and Reddy 2001; Woodard et al. 1969) of those regions and elsewhere. We provide the following diagnoses for the two species here.

Planilamina ovata n. sp.

Diagnosis. Body medium-sized, ovate, 35–70 × 30–49 μm in life; right field kineties 38–55 in number, closely packed, curving on right surface, with anterior end of leftmost kinety in right field ending at anterior one-third; left field kineties three to four in number, short, orienting left of oral region; oral cavity deep, arranged anteriorly with one (rarely two) short preoral kinety, seven to 13 infundibular kineties, and two circumoral kineties; postoral kinetofragments four, located in pocket to left of first right field kinety; contractile vacuole adjacent to cytostome, opening as a pore between second and third somatic kinety.

Type host. *Tursiops truncatus* Montagu, 1821, Atlantic bottlenose dolphin (Delphinidae); other host, *Pseudorca crassidens* Owen, 1846, false killer whale (Delphinidae).

Type locality. Marine Life Oceanarium, Gulfport, MS, USA (before Hurricane Katrina); other locality—in both *T. truncatus* and *P. crassidens* at SeaWorld Orlando, Orlando, FL, USA.

Site. In nasal tract discharge, usually accompanying *K. cetarius*, but the number in nasal mucus is usually one or two orders of magnitude fewer than that of *K. cetarius*.

Deposited specimens. Protargol-stained slide of multiple species, specimens, and stages in the Ciliate Type Slide Collection, United States Museum of Natural History, Smithsonian Institution, Washington, DC, USA, with holotype circled (USNM 1088506); additional protargol-stained paratype slide deposited in the Gulf Coast Research Laboratory Museum, The University of Southern Mississippi (GCRL 2501); additional paratype and voucher specimens remain in the senior and corresponding authors' slide collections. Note that the deposited slides also contain specimens of *K. cetarius*, which according to ICZN (1999), Article 73.3.2, are considered excluded by the authors.

Etymology. The Latin feminine adjectival name "*ovata*" refers to the typically ovate shape of the ciliate.

Planilamina magna n. sp.

Diagnosis. Body medium-sized, ovate, 57–90 × 40–63 μm in fixed and stained specimens; somatic kineties forming right and left fields; right field kineties numbering 79–99, closely packed, with anterior end of leftmost kinety in right field ending at midbody; left field kineties, three to four, adjacent to oral cavity and restricted to anterior portion of cell; oral cavity deep, arranged anteriorly and containing one short preoral kinety, three to 13 infundibular kineties, and two circumoral kineties; four postoral kinetofragments, located in pocket to left of first right field kinety.

Type host. *Pseudorca crassidens* Owen, 1846, false killer whale (Delphinidae); other host. *Tursiops truncatus* Montagu, 1821, Atlantic bottlenose dolphin (Delphinidae).

Type locality. SeaWorld Orlando, Orlando, FL, USA; other locality, Virginia Beach, VA, USA in *T. truncatus*.

Site. Nasal collection from blowhole.

Deposited specimens. Protargol-stained slide of multiple species, specimens, and stages in the Ciliate Type Slide Collection, United States Museum of Natural History, Smithsonian Institution, Washington, DC, USA, with holotype circled (USNM 1088507); protargol-stained paratype slide deposited in the Gulf Coast Research Laboratory Museum, The University of Southern Mississippi (GCRL 2502); additional paratype and voucher specimens remain in the senior and corresponding authors' slide collections. Note that slides also contain specimens of *Planilamina ovata* and *K. cetarius*, which according to ICNZ 1999, Article 73.3.2, are considered excluded by the authors. Good type specimens are circled.

Etymology. The Latin feminine adjectival name "*magna*," meaning large or great, refers to the larger size and the greater number of kineties of this species when compared with that in *Planilamina ovata*.

The subclass Phyllopharyngia according to Lynn and Small (2002) consists of two orders, Chlamydodontida and Dysteriida. Members of the former have a dorsoventrally flattened body, attaching to substratum by thigmotactic ventral cilia, and somatic cilia typically ventrally disposed in two roughly equal fields, but they have no adhesive organelle or podite; and the dysteriids typically have a laterally compressed body and an unciliated adhesive region or flexible podite. Like most members of the order Dysteriida, members of *Planilamina* not only possesses a conspicuous podite, which is a diagnostic trait of the order Dysteriida, as in *Aegyriana, Brooklynella, Dysteria, Hartmannula, Hartmannulopsis, Kyaroikeus, Microdysteria, Microxysma, Orthotrochilia, Trochilia*, and *Trochochilioides*, but members also have a heteromeric macronucleus and both preoral and circumoral kineties. As another diagnostic characteristic of Dysteriida, *Planilamina* also has CDE oriented equatorially and anteriorly at right of the rightmost kinety in right field. This structure has been given several different names, e.g. CDE (Deroux and Dragesco 1968), Fe (fragment of external kinety) and Re (right equatorial kinety) (Gong, Song, and Warren 2002), Tf (terminal fragment of kinety) (Song and Wilbert 2002), and rechte and dorsale periphere wimpernreihe (Foissner, Berger, and Kohmann 1991). Here we adopt CDE, following the earlier terminology used for this structure.

A non-ciliated strip, dorsal surface, or left side as in *Planilamina* also occurs in *Aegyriana minuta* (see Deroux 1974),

K. cetarius (see Sniezek et al. 1995), *Microxysma acutum* (see Deroux 1977), *Orthotrochilia agamalievi* (see Deroux 1977), and *Trochochilodon flavum* (see Deroux 1976).

Sniezek and Coats (1996) erected the family Kyaroikeidae to accommodate *K. cetarius* with its unique morphological and morphogenetic traits. For morphogenetic traits, *K. cetarius* and thus the family was characterized by (1) the left field not being incorporated into preexisting trophic structures, but rather arising entirely from newly formed kinetofragments; (2) cytopharyngeal reinforcements originating from circumoral kinetal anlagen rather than from independent stomatogenetic elements; and (3) the podite being derived from somatic kinetofragments rather than from right field kineties. The morphogenetic process of *Planilamina* is very similar to that of *Kyaroikeus* in the above characteristics, hence the placement of *Planilamina* in Kyaroikeidae seems reasonable. The morphogenetic pattern of *Planilamina ovata* appears to differ from that of *K. cetarius* in that (1) the postoral kinetofragments forms a 45°–90° angle to the longitudinal axis rather than being nearly parallel to it, and hence there is more counterclockwise rotation during the oral anlagen migration than occurs in *K. cetarius*; and (2) *Planilamina* usually forms three rather than four new kinetofragments to the left of parental kinetofragments at the beginning of morphogenesis.

ACKNOWLEDGMENTS

We would like to thank Dr. Connie Clemons-Chevis, Shannon Huyser, and Marci Romagnoli, previously of Marine Life Oceanarium, Gulfport, MS; Kimberly Lamey, Marie Mullen, and Tammie Henderson of Gulf Coast Research Laboratory, Ocean Springs, MS, for helping collect nasal mucus samples and preparing materials; Drs. Mike Walsh and Terry Campbell, SeaWorld of Florida; and Mr. Charlie Potter and Dr. James Meade, National Museum of Natural History, for assistance in obtaining samples. This work was supported in part by the National Marine Fisheries Service, Institute for Marine Mammal Studies Task 5; Smithsonian Marine Station as Contribution No. 651, and National Science Foundation Grant nos. 0608603 and 0529684.

LITERATURE CITED

Bandoli, J. G. & Oliverira, C. A. B. 1977. Toxoplasmose em *Sotalia guianensis* (Van Beneden, 1963), Cetacean-Delphinidae. *Folha Méd.*, **75**:459-468.

Bowater, R. O., Norton, J., Johnson, S., Hill, B., O'-Donoghue, P. & Prior, H. 2003. Toxoplasmosis in Indo-Pacific humpbacked dolphins (*Sousa chinensis*), from Queensland. *Aust. Vet. J.*, **81**:627–632.

Cruickshank, J. J., Haines, D. M., Palmer, N. C. & Staubin, K. J. 1990. Cysts of a *Toxoplasma*-like organism in an Atlantic bottlenose dolphin. *Can. Vet. J.*, **31**:213–215.

Dailey, M. D. 1985. Diseases of mammalian: Cetacea. *In*: Kinne, O. (ed.), Diseases of Marine Animals. Vol. 4. Biologisce Anstalt Helgoland, Hamburg. p. 805–847.

DeGuise, S., Lagace, A., Girard, C. & Beland, P. 1993. Intramuscular *Sarcocystis* in two beluga whales and an Atlantic white-sided dolphin from the St. Lawrence Estuary, Quebec, Canada. *J. Vet. Diagn. Invest.*, **5**:296-300.

Deroux, G. 1974. Les dispositifs adhésifs ciliaires chez les Cyrtophorida et la famille des Hypocomidae. *Protistologica*, **10**:379–396.

Deroux, G. 1976. Le plan cortical des Cyrtophorida unité d'experssion et marges de variabilité. I. Les cas des Plesiotrichopidae, fam. nov., dans la nouvelle systématique. *Protistologica*, **12**:469-481.

Deroux, G. 1977. Le plan cortical des Cyrtophorida. III. Les structures differenciatrices chez les Dysteriina. *Protistologica*, **12** (year 1976): 505–538.

Deroux, G. & Dragesco, J. 1968. Nouvelles données sur quelques ciliés holotriches cyrtophores à ciliature ventrale. *Protistologica*, **4**:365–403.

Domingo, M., Visa, J., Pumarola, M., Marco, A. J., Rabanal, R. & Kennedy, S. 1992. Pathologic and immunocytochemical studies of morbillivirus infection in striped dolphins (*Stenella coeruleoalba*). *Vet. Pathol.*, **29**:1–10.

Dubey, J. P., Zarnke, R., Thomas, N. J., Wong, S. K., Van Bonn, W., Briggs, M., Davis, J. W., Ewing, R., Mense, M., Kwok, O. C. H., Romand, S. & Thulliez, P. 2003. *Toxoplasma gondii, Neospora caninum, Sarcocystis neurona*, and *Sarcocystis canis*-like infections in marine mammals. *Vet. Parasitol.*, **116**:275–296.

Evans, D. A., Small, E. B. & Snyder, R. 1986. Investigation of ciliates collected from the baleen of fin and blue whales. Abstract booklet, Society of Protozoologists, 39th Annual Meeting, Kingston, RI., Abstract #5

Ewing, R., Zaias, J., Stamper, M. A., Bossart, G. D. & Dubey, J. P. 2002. Prevalence of *Sarcocystis* sp. in stranded Atlantic white-sided dolphins (*Lagenorhynchus acutus*). *J. Wildlife Dis.*, **38**:291–296.

Foissner, W., Berger, H. & Kohmann, F. 1991. Taxonomische und ökoligische Revision der Ciliaten des Saprobiensystems-Band 1: Cryrtophorida, Oligotrichida, Hypotrichida, Colpodea. *Inf. Bayer. Landesamtes Wasserwirtsch.*, **1/92**:1-478.

Gong, J., Song, W. & Warren, A. 2002. Redescriptions of two marine cyrtophorid ciliates, *Dysteria cristata* (Gourret and Roeser, 1888) Kahl, 1931 and *Dysteria monostyla* (Ehrenberg, 1838) Kahl, 1931 (Protozoa, Ciliophora, Cyrtophorida), from China. *Europ. J. Protistol.*, **38**: 213–222.

Howard, E. B., Britt, J. O. & Matsumoto, G. K. 1983. Parasitic diseases. *In*: Howard, E. B. (ed.), Pathobiology of Marine Mammal Diseases. Vol. 1. CRC Press, Boca Raton. p. 119–232.

International Commission on Zoological Nomenclature. 1999. International Code of Zoological Nomenclature. 4th ed. The International Trust for Zoological Nomenclature, The Natural History Museum, London. p. 81–82.

Jardine, J. E. & Dubey, J. P. 2002. Congenital toxoplasmosis in an Indo-Pacific bottlenose dolphin (*Tursiops aduncus*). *J. Parasitol.*, **88**: 197–199.

Lapointe, J. M., Duignan, P. J., Marsh, A. E., Gulland, F. M., Barr, C., Nayden, D. K., King, D. P., Farman, C. A., Burek Huntingdon, K. A. & Lowenstein, L. J. 1998. Meningoencephalitis due to a *Sarcocystis neurona*-like protozoan in Pacific harbor seals (*Phoca vitulina richardsi*). *J. Parasitol.*, **84**:1184–1189.

Lynn, D. H. & Small, E. B. 2002. Phylum Ciliophora, Doflein, 1901. *In*: Lee, J. J., Leedale, G. F. & Bradbury, P. (ed.), An Illustrated Guide to the Protozoa. 2nd ed. Society of Protozoologists, Lawrence. p. 371–656.

Migaki, G., Sawa, T. R. & Dubey, J. P. 1990. Fatal disseminated toxoplasmosis in a Spinner dolphin (*Stenella longirostris*). *Vet. Pathol.*, **27**:463-464.

Mikaelian, I., Boisclair, J., Dubey, J. P., Kennedy, S. & Martineau, D. 2000. Toxoplasmosis in beluga whales (*Delphinapterus leucas*) from the St. Lawrence Estuary: two case reports and a serological survey. *J. Comp. Pathol.*, **122**:73–76.

Montagnes, D. J. & Lynn, D. H. 1993. A quantitative protargol stain (QPS) for ciliates and other protists. *In*: Kemp, P. F. et al. (ed.), Handbook of Methods in Aquatic Microbial Ecology. Lewis Publishers, Boca Raton. p. 22–240.

Oksanen, A., Tryland, M., Johnsen, K. & Dubey, J. P. 1998. Serosurvey of *Toxoplasma gondii* in North Atlantic marine mammals by the use of agglutination test employing whole tachyzoites and dithiothreitol. *Comp. Immunol. Microbiol. Infect. Dis.*, **21**:107–114.

Poynton, S. L., Whitaker, B. R. & Heinrich, A. B. 2001. A novel trypanoplasm-like flagellate *Jarrellia atramenti* n. g., n. sp. (Kinetoplastida: Bodonidae) and ciliates from the blowhole of a stranded pygmy sperm whale *Kogia breviceps* (Physeteridae): morphology, life cycle and potential pathogenicity. *Dis. Aquat. Org.*, **44**:191–201.

Resendes, A. R., Juan, S. C., Almeria, S., Majo, N., Domingo, M. & Dubey, J. P. 2002b. Hepatic sarcocystosis in a striped dolphin (*Stenella coeruleoalba*) from the Spanish Mediterranean coast. *J. Parasitol.*, **88**:206–209.

Resendes, A. R., Almeria, S., Dubey, J. P., Obon, E., Juan, S. C., Degollada, E., Alegre, F., Cabezon, O., Pont, S. & Domingo, M. 2002a. Disseminated toxoplasmosis in a Mediterranean pregnant Risso's dolphin (*Grampus griseus*) with transplacental fetal infection. *J. Parasitol.*, **88**:1029–1032.

Schulman, F. Y. & Lipscomb, T. P. 1997. Ciliate dermatitis in dolphins that died during 1987–88 Atlantic bottlenose dolphin morbilliviral epizootic. *Vet. Pathol.*, **36**:171–174.

Schulman, F. Y. & Lipscomb, T. P. 1999. Dermatitis with invasive ciliated protozoa in dolphins that died during the 1987–1988 Atlantic bottlenose dolphin morbilliviral epizootic. *Vet. Pathol.*, **34**:505.

Sniezek, J. H. & Coats, D. W. 1996. Stomatogenesis in *Kyaroikeus cetarius* (Dysteriina, Kyaroikeidae, n. fam.): clues to its systematic placement. *J. Eukaryot. Microbiol.*, **43**:111–119.

Sniezek, J. H., Coats, D. W. & Small, E. B. 1995. *Kyaroikeus cetarius* n. g., n. sp.: a parasitic ciliate from the respiratory tract of odonticete cetacean. *J. Eukaryot. Microbiol.*, **42**:260–268.

Song, W. & Wilbert, N. 2002. Faunistic studies on marine ciliates from the Antarctic benthic area, including descriptions of one epizoic form, 6 new species, and 2 new genera (Protozoa: Ciliophora). *Acta Protozool.*, **41**:23–61.

Sweeney, J. C. & Reddy, M. L. 2001. Cetacean cytology. *In*: Dierauf, L. A. & Gulland, F. M. D. (ed.), Marine Mammal Medicine. 2nd ed. CRC Press, New York. p. 437–448.

Wilbert, N. 1975. Eine verbesserte technik der protargolimpânation-für ciliaten. *Mikrokosmos*, **64**:171–179.

Woodard, J. C., Zam, S. G., Caldwell, D. K. & Caldwell, M. C. 1969. Some parasitic diseases of dolphins. *Pathol. Vet.*, **6**:257–272.

Woodcock, H. M. & Lodge, O. 1921. British Antarctic (''Terra Nova'') Expedition, 1910. Natural history report. Protozoa. Part I. Parasitic Protozoa. *Br. Mus. (Nat. Hist.) Rep. Zool.*, **6**:1–24.

Received: 03/14/06, 05/22/06; accepted: 05/23/06